RAA 2018 Vol. **18** No. **7**, 78(8pp) doi: 10.1088/1674–4527/18/7/78

http://www.raa-journal.org *http://iopscience.iop.org/raa*

Research in Astronomy and Astrophysics

PS Vir: a short-period solar-like contact binary

Hui-Yu Yuan[1], Hai-Feng Dai[2] and Yuan-Gui Yang[1,2]

[1] Information College, Huaibei Normal University, 235000 Huaibei, China
[2] School of Physics and Electronic Information, Huaibei Normal University, 235000 Huaibei, China; *yygcn@163.com*

Received 2018 February 24; accepted 2018 April 4

Abstract We present multi-color photometric observations and a one-dimensional spectrum, acquired from March 2016 to May 2017, for the short-period eclipsing binary PS Vir, by using the 2.16-m, 85-cm and 60-cm telescopes at Xinglong station, which is administered by National Astronomical Observatories, Chinese Academy of Sciences. The spectral type was determined as G2V from the one-dimensional spectrum. The photometric solution was reduced from BVR_c light curves. The results imply that PS Vir is a W-subtype contact binary with a mass ratio of $q = 0.305(\pm 0.008)$ and a fill-out factor of $f = 14.4(\pm 1.8)\%$. The orbital period may be undergoing a cyclic oscillation with an amplitude of $A = 0.0027(\pm 0.0001)$ d and a modulated period of $11.7(\pm 0.2)$ yr, which may result from the light-time effect due to a third body. The lower limit on mass for the assumed component is $0.12\,M_\odot$. Moreover, the more massive component of PS Vir may be a bit more evolved star as determined from the mass-luminosity diagram.

Key words: binaries: close — binaries: eclipsing — stars: individual (PS Vir) — stars

1 INTRODUCTION

W UMa contact binaries (i.e., EW-type) are eclipsing systems in which both stars overflow their Roche lobes, sharing a common envelope (Lucy 1968). They are formed from nearly normal main-sequence stars with spectral types usually between F and K. Their light amplitudes are usually < 0.8 mag in the V band and the depths of both eclipsing minima are almost equal (Samus et al. 2017), implying that the two components possess almost identical temperatures. The mass ratio generally ranges from 0.2 to 0.5, but reported values are almost as high as unity for GU Mon (Lorenzo et al. 2016) and as low as 0.065 for V857 Her (Qian et al. 2005). The extreme mass ratio may preliminarily be $0.044(\pm 0.007)$ from a statistical analysis of 46 deep, low mass ratio overcontact binaries (Yang & Qian 2015). The orbital periods are usually smaller than one day. According to the newest statistics based on LAMOST data (Qian et al. 2017), the peak of the period distribution is near 0.29 d, and the short-period cut-off is at 0.2 d. Although EW-type binaries have recently been detected by several surveys, i.e., the Robotic Optical Transient Search Experiment (ROTSE; Akerlof et al. 2000), the Optical Gravitational Lensing Experiment (OGLE; Szymanski et al. 2001) and the All Sky Automated Survey (ASAS; Pojmanski 2002), high-precision photometry and spectroscopy for individual stars are necessitated in order to study their intrinsic light variability, such as exhibited by DZ Psc (Yang et al. 2013) and V410 Aur (Luo et al. 2017), and determine their absolute parameters.

PS Vir (= GSC 00279–00321) is a W UMa-type binary as determined by automated variable star classification using the Northern Sky Variability Survey (Woźniak et al. 2004). Hoffman et al. (2009) obtained an orbital period of 0.28982 d and a light variability amplitude of 0.423 mag by the Fourier analysis method. From the VizieR Online Data Catalog[3], the magnitude and colors for this star are $J = 10.719(\pm 0.021)$ mag, $J - H = 0.428(\pm 0.022)$ mag and $H - K = 0.066(\pm 0.021)$ mag. From the characteristic shape of its

[3] *http://vizier.cfa.harvard.edu/viz-bin/VizieR?-source=II/246*

light curve, Koppelman & Terrell (2002) identified it as a W UMa binary using their unfiltered observations. This binary system shows a large asymmetry of about 0.1 mag between maxima, which may be attributed to X-ray emission arising from coronal activity.

In the present paper, we describe the observational data and related reductions for PS Vir in Section 2, where the complete light curves and one-dimensional spectrum are also presented. Two possible period studies are listed in Section 3, and we model BVR_c light curves in Section 4. Finally, we give some discussions including the evolutionary state and interpretations of the possible period variations in Section 5.

2 OBSERVATIONS

2.1 Spectroscopy

The spectrum of PS Vir was taken at Xinglong station (XLS), which is administered by National Astronomical Observatories, Chinese Academy of Sciences (NAOC), with the Beijing-Faint Object Spectrograph and Camera (BFOSC) attached to the 2.16-m telescope. We chose a $1.8''$ slit and a *Grism-3* with a wavelength range from 3300 Å to 6400 Å. The exposure time of 600 s started at UT=12:26:10.3 on 2017 June 7 (i.e., Heliocentric Julian Date (HJD) 2457941.0182). We extracted the one-dimensional spectrum and calibrated its wavelength according to the spectral atlas of BFOSC wavelength calibration lamps[4], after performing reduction including bias subtraction, flat-fielding and cosmic-ray removal by IRAF packages. From the spectrum for PS Vir, it is easy to find some characteristic spectral lines, such as CaII (3934 Å and 3968 Å), CaI (4227 Å), Hδ (4101 Å), Hβ (4861 Å) and G-band (4308 Å), which are shown in Figure 1. Comparing the spectrum of PS Vir with the spectra in the stellar spectral flux library (Pickles 1998), we determined the spectral type of G2V by using the winmk software[5].

2.2 CCD Photometry

New photometry of PS Vir was carried out on 2016 March 23, 24 and 27 with the 60-cm telescope (Yang et al. 2010), and on 2017 April 30 and May 1 with the 85-cm telescope (Zhou et al. 2009) at XLS. Those two telescopes are both equipped with the standard Johnson-Cousins-Bessel $UBVR_cI_c$ systems. All effective CCD images were reduced by using the IMRED and APPHOT packages of IRAF in standard mode. Differential magnitudes between the variable and comparison stars were obtained by aperture photometry.

In the observation process, TYC 0279-0536-1 and 2MASS J11573732+0620392 were chosen as comparison and check stars respectively. In March 2016, we obtained a set of complete light curves, as shown in Figure 2(a). The exposure times were 40 s for B, 20 s for V and 10 s for R_c band. The individual magnitude differences *versus* HJD (i.e., Δm vs. HJD) are available upon request. The standard derivations are estimated to be ± 0.024 mag in B, ± 0.017 mag in V and ± 0.026 mag in R. From Figure 2(a), the multi-color light curves indicate that PS Vir may be a W UMa-type eclipsing binary. The large asymmetry of about 0.1 mag between both maxima (Koppelman & Terrell 2002) disappears in the new light curves.

On 2017 April 30 and May 1, moreover, two eclipses for PS Vir were observed as displayed in Figure 2(b). Using our new observations together with data from Koppelman & Terrell (2002), we determined several light minimum times, which are listed in Table 1 including their observed errors and measurement methods.

3 ORBITAL PERIOD VARIATIONS

In order to study the period changes for PS Vir, we compile all available eclipsing times from the $O-C$ gateway[6]. All those data with their errors are listed in Table 2, including two photoelectric and 23 CCD measurements.

In the calculation process, the individual weights are given inversely proportional to their uncertainties. The orbital period of PS Vir is updated to be as follows,

$$\begin{aligned} \text{Min.I} = & \text{ HJD } 2452425.7321(11) \\ & +0.28980595(9) \times E, \end{aligned} \quad (1)$$

where the numbers in brackets express errors in the last decimal place. Based on Equation (1), we obtained the initial residuals, $(O-C)_i$, which are listed in Table 2 and also shown in the upper panels of Figure 3.

From this figure, we easily find that the $(O-C)_i$ curve may be described as an upward parabola, which implies the existence a long-term period increase. This

[4] *http://www.xinglong-naoc.org/html/tzgg/detail-6.html*

[5] *http://www.appstate.edu/∼grayro/MK/winmk.htm*

[6] *http://var2.astro.cz/ocgate/?lang=en*

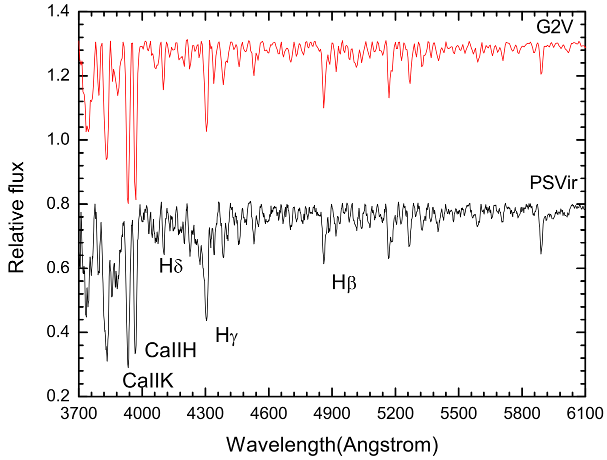

Fig. 1 Spectrum of PS Vir and an example of a G2V spectral type.

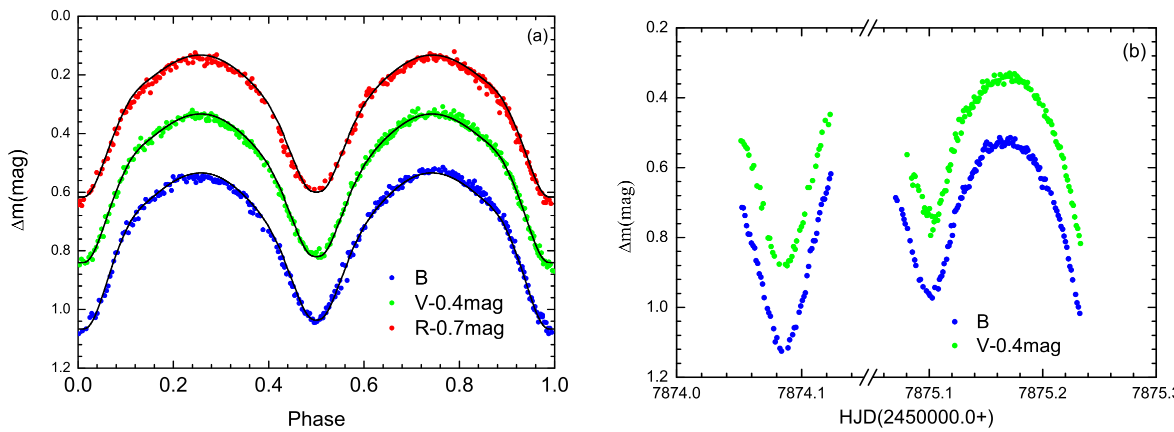

Fig. 2 BVR_c light curves (a) and two eclipses (b) for the eclipsing binary PS Vir, observed by using the 60-cm and 85-cm telescopes, respectively. The computed light curves are plotted as continuous *black lines* by the photometric solution.

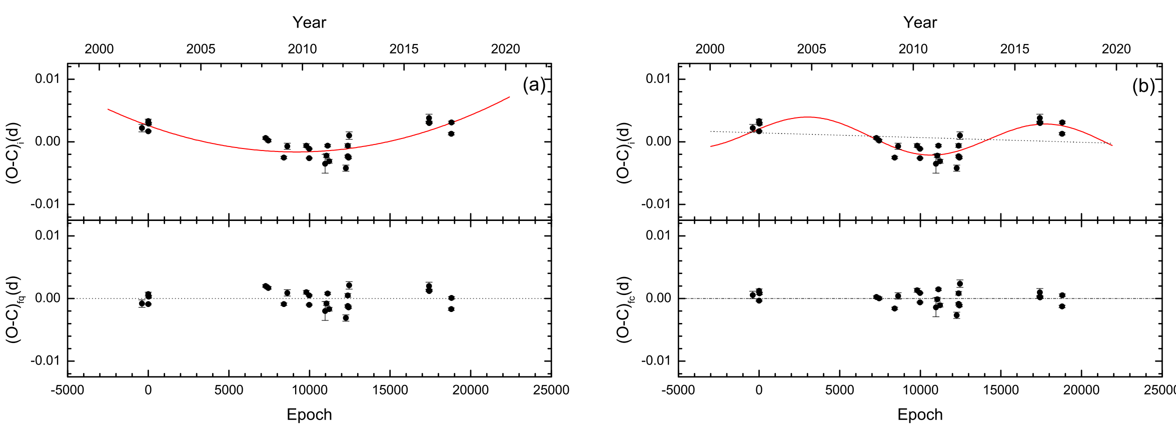

Fig. 3 The $(O-C)$ diagrams for PS Vir. The *solid circles* represent photoelectric and CCD data. The continuous *red lines* in both upper panels are plotted by Equation (2) and Equation (3), respectively.

yields the following equation,

$$(O-C)_i = +0.0026(\pm 0.0001) - 9.2(\pm 0.1)\times 10^{-7}\times E + 5.01(\pm 0.53)\times 10^{-11}\times E^2. \qquad (2)$$

The corresponding residuals, $(O-C)_q$, are listed in Table 2 and are also displayed in the lower panel of Figure 3(a). The value of χ^2/N from Equation (2) is 29.2. From the coefficient of the quadratic term, a period

Table 1 New Light Minimum Times of PS Vir

HJD	Error	Min.	Filter	Telescope
2457471.25747	±0.00016	I	B	60-cm
2457471.25745	±0.00017	I	V	60-cm
2457471.25694	±0.00019	I	R	60-cm
2457472.27085	±0.00015	II	B	60-cm
2457472.27149	±0.00018	II	V	60-cm
2457472.27104	±0.00022	II	R	60-cm
2457475.16894	±0.00012	II	B	60-cm
2457475.16912	±0.00015	II	V	60-cm
2457475.16921	±0.00019	II	R	60-cm
2457874.08541	±0.00020	I	B	85-cm
2457874.08521	±0.00017	I	V	85-cm
2457875.10064	±0.00014	II	B	85-cm
2457875.10215	±0.00027	II	V	85-cm
2452313.86998*	±0.00079	I	V	IBVS5299
2452313.86867*	±0.00049	I	I_c	IBVS5299
2452425.73392*	±0.00015	I	no	IBVS5299
2452426.74984*	±0.00026	II	no	IBVS5299
2452431.67610*	±0.00023	II	no	IBVS5299

Table 2 All Compiled Light Minimum Times for PS Vir

HJD	Error	Epoch	Type	Method	$(O-C)_i$ (d)	$(O-C)_q$ (d)	$(O-C)_c$ (d)	Ref.
2452313.8693	±0.0006	−386.0	I	CCD	+0.0022	−0.0008	+0.0006	[1]
2452425.7339	±0.0001	+0.0	I	CCD	+0.0017	−0.0009	−0.0004	[1]
2452426.7498	±0.0003	3.5	II	CCD	+0.0033	+0.0007	+0.0012	[1]
2452431.6761	±0.0002	20.5	II	CCD	+0.0029	+0.0003	+0.0008	[1]
2454535.5201	±0.0002	7280.0	I	CCD	+0.0006	+0.0020	+0.0002	[2]
2454583.3377	±0.0002	7445.0	I	CCD	+0.0002	+0.0017	+0.0000	[2]
2454863.8671	±0.0002	8413.0	I	CCD	−0.0025	−0.0009	−0.0016	[3]
2454924.4384	±0.0005	8622.0	I	CCD	−0.0007	+0.0009	+0.0004	[4]
2455267.7136	±0.0003	9806.5	II	CCD	−0.0006	+0.0010	+0.0013	[5]
2455318.2827	±0.0001	9981.0	I	CCD	−0.0026	−0.0010	−0.0006	[6]
2455318.4291	±0.0001	9981.5	II	CCD	−0.0011	+0.0005	+0.0009	[6]
2455605.9142	±0.0015	10973.5	II	CCD	−0.0035	−0.0020	−0.0014	[7]
2455629.3898	±0.0003	11054.5	II	pe	−0.0022	−0.0008	−0.0001	[8]
2455650.4024	±0.0002	11127.0	I	pe	−0.0006	+0.0008	+0.0015	[9]
2455677.7865	±0.0003	11221.5	II	CCD	−0.0031	−0.0017	−0.0011	[7]
2455978.8938	±0.0005	12260.5	II	CCD	−0.0042	−0.0031	−0.0027	[10]
2456011.3540	±0.0002	12372.5	II	CCD	−0.0023	−0.0012	−0.0009	[11]
2456011.5006	±0.0003	12373.0	I	CCD	−0.0006	+0.0005	+0.0008	[11]
2456026.7135	±0.0002	12425.5	II	CCD	−0.0025	−0.0014	−0.0011	[12]
2456036.7153	±0.0006	12460.0	I	CCD	+0.0010	+0.0021	+0.0024	[10]
2457471.2575	±0.0006	17410.0	I	CCD	+0.0038	+0.0020	+0.0010	[1]
2457472.2711	±0.0002	17413.5	II	CCD	+0.0031	+0.0013	+0.0003	[1]
2457475.1691	±0.0001	17423.5	II	CCD	+0.0030	+0.0012	+0.0002	[1]
2457874.0853	±0.0002	18800.0	I	CCD	+0.0013	−0.0017	−0.0013	[1]
2457875.1014	±0.0002	18803.5	II	CCD	+0.0031	+0.0001	+0.0005	[1]

Notes: [1] Present paper; [2] Brát et al. (2008); [3] Diethelm (2009); [4] Brat et al. (2009); [5] Diethelm (2010); [6] Demircan et al. (2011); [7] Diethelm (2011); [8] Hubscher & Lehmann (2013); [9] Hoňková et al. (2013); [10] Diethelm (2012); [11] Gursoytrak et al. (2013); [12] Nelson (2013).

increase rate is computed to be

$$dP/dt = +1.26(\pm 0.13) \times 10^{-7}\,\mathrm{d\,yr^{-1}}\,.$$

Equation (2) is plotted as a solid line in the upper panel of Figure 3(a).

As is apparent in Figure 3, there exists a gap between HJD 2452431.6761 (i.e. Epoch = 20.5; Koppelman & Terrell 2002) and HJD 2454535.5201 (i.e. Epoch = 7280.0; Brát et al. 2008) up to about 18 yr. We assume that the parabolic curve may be part of a sine curve. Therefore, the residuals $(O-C)_i$ are fitted by a linear and sinusoidal ephemeris. By using a nonlinear weighted least-squares method, we obtain the following equation,

$$(O-C)_i = 0.0014(\pm0.0002) + 0.0027(\pm0.0001) \times \sin[4.26(\pm0.07)\times10^{-5}\times E + 0.228(\pm0.065)]. \quad (3)$$

The corresponding residuals, $(O-C)_c$, are also listed in Table 2 and shown in the lower panel of Figure 3(b). The value of χ^2/N from Equation (3) is 18.1. The solid line in the upper panel of Figure 3(b) is described by Equation (3). By using the relation $P_{\rm mod} = 2\pi P/\omega$ with $\omega = 4.26(\pm0.07)$ and $P = 0.28980595(9)\,{\rm d}$, a modulated period of $P_{\rm mod} = 11.7(\pm0.2)\,{\rm yr}$ can be computed. This kind of case is similar to our previously studied binaries WY Tau (Yang 2009) and AR Dra (Yang et al. 2016). The small value of χ^2/N from Equation (3) may imply that it represents the true period changes although this needs to be checked in future observations.

4 MODELING LIGHT CURVES

The photometric solution for PS Vir is deduced from BVR_c light curves acquired in 2016 by the updated version of the Wilson-Devinney program (Wilson & Devinney 1971; Wilson 1979; Wilson & van Hamme 2014 [7], including Kurucz (1993)'s stellar atmosphere model. The albedos and gravity darkening coefficients are set to be $A_{\rm p,s} = 0.5$ (Ruciński 1973) and $g_{\rm p,s} = 0.32$ (Lucy 1967) respectively, which are appropriate for stars with convective envelopes. Following van Hamme (1993), we determined the logarithmic bolometric (i.e., X and Y) and monochromatic limb-darkening coefficients (i.e., x and y), which are based on the effective temperatures of the stars. During the calculation, the adjustable parameters are listed as follows: i, q, $T_{\rm s}$, $\Omega_{\rm p,s}$, $L_{\rm p}$ and l_3.

Based on the spectral type of G2V, we adopted the effective temperature for the primary component to be $T_{\rm p} = 5800(\pm80)\,{\rm K}$ (Cox 2000). As shown in Figure 2(a), the three color light curves for PS Vir include 319 data points in B, 341 data points in V and 293 data points in R_c, which are simultaneously used to obtain the photometric elements. The calculation always uses Mode 3 (i.e., contact configuration). Due to lack of a spectroscopic mass ratio, we firstly search for a mass ratio, which ranges from 0.2 to 4.4 with a step of 0.1. After performing a series of solutions with fixed mass ratios, we obtained the relation of q and $\Sigma(O-C)_i^2$, which is displayed in Figure 4. From this figure, we located a minimum value of $\Sigma(O-C)_i^2$ around $q = 3.4$, which implies that PS Vir is a W-subtype for this contact binary. Then we considered q and l_3 as free parameters. At last we identified the best photometric solution, which is listed in Table 3.

The computed light curves are constructed as solid lines in Figure 2(a). The third lights in BVR_c bands are $l_{3B} = 0.42\%$, $l_{3V} = 0.30\%$ and $l_{3R} = 0.33\%$, respectively. The mass ratio and fill-out factor for this binary are $q_{\rm ph} = 0.305(\pm0.008)$ and $f = 14.4(\pm1.5)\%$, respectively. Therefore, PS Vir is a short-period solar-like shallow contact binary. It resembles another two binaries, DD Com (Zhu et al. 2010) and AD Cnc (Qian et al. 2007), whose periods can show increase, decrease and cyclic change.

5 DISCUSSION

From the previous analysis, we deduced the photometric solution with a weak third light for BVR_c light curves. The orbital period of PS Vir may be undergoing a secular period increase or a periodic oscillation. Due to the small value of χ^2/N, Equation (3) is accepted to be the final result for period variations, which is similar to other eclipsing binaries such as WW Dra (Liao & Qian 2010), BI Vul (Qian et al. 2013), IR Cas (Zhu et al. 2004), V401 Cyg (Zhu et al. 2013) and V1191 Cyg (Zhu et al. 2011). Based on the G2V-type star, we estimated the mass of the more massive component to be $M_{\rm p} = 1.00(\pm0.03)\,M_\odot$ (Cox 2000), whose error results from an uncertainty in spectral subtype. Combining the photometric elements, we can determine other absolute parameters, which are listed in Table 4. In order to analyze the evolutionary status of PS Vir, we construct the mass-luminosity diagram in Figure 5.

The zero-age main sequence (ZAMS) and the terminal-age main sequence (TAMS) are computed by the binary-star evolution code (i.e., BSE, Hurley et al. 2002). From Figure 5, the more massive component of PS Vir is between the ZAMS and TAMS lines, which implies that it may be an evolved star. Meanwhile, the less massive star lies above the TAMS line. This may result from energy transfer from the primary to the secondary,

[7] *ftp://ftp.astro.ufl.edu/pub/wilson/lcdc2015*

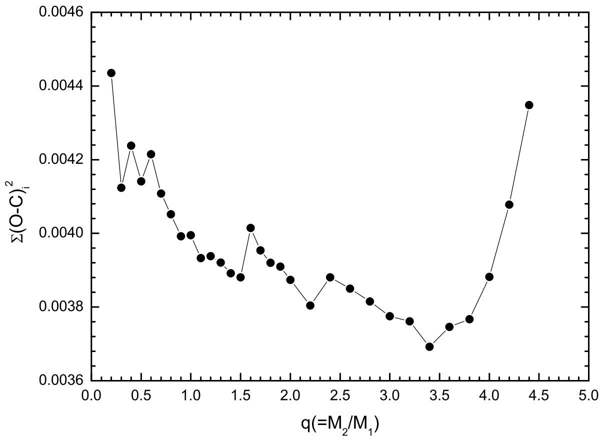

Fig. 4 The relation between q and Σ for PS Vir.

Table 3 Photometric Elements of the Contact Binary PS Vir

Parameter	Primary	Secondary
$i(°)$	79.8($\pm$0.3)	
$q = M_{\rm p}/M_{\rm s}$	0.305($\pm$0.008)	
T (K)	5800($\pm$80)	5976($\pm$8)
X, Y	$+0.649$, $+0.220$	$+0.660$, $+0.210$
x_B, y_B	$+0.837$, $+0.158$	$+0.830$, $+0.187$
x_V, y_V	$+0.761$, $+0.238$	$+0.749$, $+0.257$
x_R, y_R	$+0.669$, $+0.254$	$+0.657$, $+0.267$
$\Omega_{\rm p} = \Omega_{\rm s}$	2.4505($\pm$0.0034)	
$L/(L_{\rm p}+L_{\rm s})_B$	0.7074($\pm$0.0018)	0.2926($\pm$0.0018)
$L/(L_{\rm p}+L_{\rm s})_V$	0.7169($\pm$0.0016)	0.2831($\pm$0.0017)
$L/(L_{\rm p}+L_{\rm s})_R$	0.7225($\pm$0.0024)	0.2776($\pm$0.0024)
$l_{3B}^{\star}$	0.42($\pm$0.05)%	
$l_{3V}^{\star}$	0.30($\pm$0.05)%	
$l_{3R}^{\star}$	0.33($\pm$0.07)%	
r (pole)	0.4604($\pm$0.0005)	0.2688($\pm$0.0003)
r (side)	0.4963($\pm$0.0005)	0.2808($\pm$0.0003)
r (back)	0.5235($\pm$0.0006)	0.3187($\pm$0.0004)
f	14.4($\pm$1.8)%	

Notes: * The third light l_3 is $L_3/(L_1+L_2+L_3)$.

Table 4 Absolute Parameters and Related Deduced Values for PS Vir

Parameter	Primary	Secondary
a (AU)	2.01($\pm$0.03)	
M ($M_\odot$)	1.00($\pm$0.03)	0.31($\pm$0.02)
R ($R_\odot$)	1.10($\pm$0.03)	0.58($\pm$0.02)
L ($L_\odot$)	1.24($\pm$0.06)	0.39($\pm$0.02)
$\Delta P/P$	3.97($\pm$0.15) $\times 10^{-6}$	
ΔQ ($\times 10^{49}$ g cm^2)	1.72($\pm$0.07)	0.53($\pm$0.02)
$a_{12} \sin i'$ (AU)	0.467($\pm$0.017)	
$f(m)$ ($M_\odot$)	7.46($\pm$0.83) $\times 10^{-4}$	

which is similar to other W-subtype low temperature contact binaries (LTCBs) (Yakut & Eggleton 2005).

For eclipsing binaries, the observed period oscillations may be interpreted as either cyclic magnetic activity (Applegate 1992) or the light-time effect via the presence of a third body (Irwin 1952). Applegate (1992) pointed out that the period oscillation may be contributed by magnetic activity cycles through variations in the gravita-

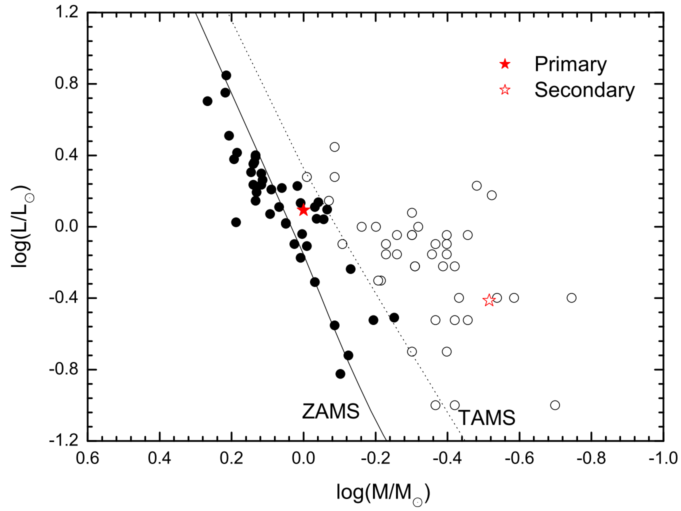

Fig. 5 Mass-luminosity diagram for PS Vir. The *solid* and *open circles* refer to the primary and secondary components for the W-subtype LTCBs, respectively (Yakut & Eggleton 2005).

tional quadrupole moment, ΔQ, for one or both components. With the relation $\Delta Q = -9Ma^2\Delta P/P$ (Lanza & Rodonò 2002), variations in the quadruple moment ΔQ for both components are computed, and are also listed in Table 4. For a contact binary, the typical value of ΔQ is of the order of 10^{51}–10^{52} (Lanza & Rodonò 1999). Values of $\Delta Q_{\rm p,s}$ from Table 4 are evidently much smaller than the typical values. Therefore, we can disregard this mechanism in the binary PS Vir.

Another possible mechanism is the light-time effect due to a third body, which may result in cyclic variations. With the fitting parameters in Equation (3), we can easily obtain a mass function of $f(m) = 7.46(\pm 0.83) \times 10^{-4}\,M_\odot$ for the assumed third body. Finally, we can obtain the minimum mass of $M_3 = 0.12(\pm 0.1)\,M_\odot$ at $a_{12} = 5.3(\pm 0.4)$ AU. This effect may be efficient for detecting low mass objects such as substellar objects in NN Ser (Qian et al. 2009) and HU Aqr (Qian et al. 2011). Such low-mass dwarfs are difficult to find based on direct evidence due to their extremely low luminosity, which is weakly identified by the third light in Table 3 (i.e., $l_3 < 0.5\%$). However, the small values of $\Delta Q_{\rm p,s}$ imply that Applegate's magnetic mechanism may not work. The observed periodic oscillation may result from the light-time effect via the presence of an additional component, which implies that PS Vir may be a triple star. This may provide observational evidence that contact binary stars exist in multiple systems (D'Angelo et al. 2006; Pribulla & Rucinski 2006; Rucinski et al. 2007). Future observations should obtain high-precision photometry and spectroscopy in order to check the period changes and to determine the associated absolute parameters.

Acknowledgements Research leading to these results has received funding from the National Natural Science Foundation of China (Nos. 11473009 and U1231102), and the Outstanding Young Talents Program of the Education Department of Anhui Province (No. gxyq2018161). Many thanks are given to the anonymous referee for his/her constructive comments and helpful suggestions. We acknowledge support from the staff at the Xinglong 2.16-m/85-cm/60-cm telescopes. This work was partially supported by the Open Project Program of the Key Laboratory of Optical Astronomy, National Astronomical Observatories, Chinese Academy of Sciences.

References

Akerlof, C., Amrose, S., Balsano, R., et al. 2000, AJ, 119, 1901
Applegate, J. H. 1992, ApJ, 385, 621
Brát, L., Šmelcer, L., Kuèáková, H., et al. 2008, Open European Journal on Variable Stars, 94, 1
Brat, L., Trnka, J., Lehky, M., et al. 2009, Open European Journal on Variable Stars, 107, 1
Cox, A. N. 2000, Allen's astrophysical quantities (New York: AIP Press; Springer)
D'Angelo, C., van Kerkwijk, M. H., & Rucinski, S. M. 2006, AJ, 132, 650
Demircan, Y., Gurol, B., Gokay, G., et al. 2011, Information Bulletin on Variable Stars, 5965, 1

Diethelm, R. 2009, Information Bulletin on Variable Stars, 5894, 1

Diethelm, R. 2010, Information Bulletin on Variable Stars, 5945, 1

Diethelm, R. 2011, Information Bulletin on Variable Stars, 5992, 1

Diethelm, R. 2012, Information Bulletin on Variable Stars, 6029, 1

Gursoytrak, H., Demircan, Y., Gokay, G., et al. 2013, Information Bulletin on Variable Stars, 6075

Hoffman, D. I., Harrison, T. E., & McNamara, B. J. 2009, AJ, 138, 466

Hoňková, K., Juryšek, J., Lehký, M., et al. 2013, Open European Journal on Variable Stars, 160, 1

Hubscher, J., & Lehmann, P. B. 2013, Information Bulletin on Variable Stars, 6070, 1

Hurley, J. R., Tout, C. A., & Pols, O. R. 2002, MNRAS, 329, 897

Irwin, J. B. 1952, ApJ, 116, 211

Koppelman, M. D., & Terrell, D. 2002, Information Bulletin on Variable Stars, 5299, 1

Kurucz, R. L. 1993, in Astronomical Society of the Pacific Conference Series, 44, IAU Colloq. 138: Peculiar versus Normal Phenomena in A-type and Related Stars, eds. M. M. Dworetsky, F. Castelli, & R. Faraggiana, 87

Lanza, A. F., & Rodonò, M. 1999, A&A, 349, 887

Lanza, A. F., & Rodonò, M. 2002, A&A, 390, 167

Liao, W.-P., & Qian, S.-B. 2010, MNRAS, 405, 1930

Lorenzo, J., Negueruela, I., Vilardell, F., et al. 2016, A&A, 590, A45

Lucy, L. B. 1967, ZAp, 65, 89

Lucy, L. B. 1968, ApJ, 151, 1123

Luo, X., Wang, K., Zhang, X., et al. 2017, AJ, 154, 99

Nelson, R. H. 2013, Information Bulletin on Variable Stars, 6050, 1

Pickles, A. J. 1998, PASP, 110, 863

Pojmanski, G. 2002, Acta Astronomica, 52, 397

Pribulla, T., & Rucinski, S. M. 2006, AJ, 131, 2986

Qian, S.-B., Zhu, L.-Y., Soonthornthum, B., et al. 2005, AJ, 130, 1206

Qian, S.-B., Yuan, J.-Z., Soonthornthum, B., et al. 2007, ApJ, 671, 811

Qian, S.-B., Dai, Z.-B., Liao, W.-P., et al. 2009, ApJ, 706, L96

Qian, S.-B., Liu, L., Liao, W.-P., et al. 2011, MNRAS, 414, L16

Qian, S.-B., Liu, N.-P., Li, K., et al. 2013, ApJS, 209, 13

Qian, S.-B., He, J.-J., Zhang, J., et al. 2017, RAA (Research in Astronomy and Astrophysics), 17, 087

Ruciński, S. M. 1973, Acta Astronomica, 23, 79

Rucinski, S. M., Pribulla, T., & van Kerkwijk, M. H. 2007, AJ, 134, 2353

Samus, N. N., Kazarovets, E. V., Durlevich, O. V., Kireeva, N. N., & Pastukhova, E. N. 2017, Astronomy Reports, 61, 80

Szymanski, M., Kubiak, M., & Udalski, A. 2001, Acta Astronomica, 51, 259

van Hamme, W. 1993, AJ, 106, 2096

Wilson, R. E. 1979, ApJ, 234, 1054

Wilson, R. E., & van Hamme, W. 2014, ApJ, 780, 151

Wilson, R. E., & Devinney, E. J. 1971, ApJ, 166, 605

Woźniak, P. R., Vestrand, W. T., Akerlof, C. W., et al. 2004, AJ, 127, 2436

Yakut, K., & Eggleton, P. P. 2005, ApJ, 629, 1055

Yang, Y.-G. 2009, PASJ, 61, 1211

Yang, Y.-G., Dai, H.-F., & Yin, X.-G. 2010, New Astron., 15, 392

Yang, Y.-G., Qian, S.-B., Zhang, L.-Y., Dai, H.-F., & Soonthornthum, B. 2013, AJ, 146, 35

Yang, Y.-G., & Qian, S.-B. 2015, AJ, 150, 69

Yang, Y.-G., Dai, H.-F., Zhou, Z., & Li, Q. 2016, AJ, 151, 124

Zhou, A.-Y., Jiang, X.-J., Zhang, Y.-P., & Wei, J.-Y. 2009, RAA (Research in Astronomy and Astrophysics), 9, 349

Zhu, L.-Y., Qian, S.-B., & Xiang, F.-Y. 2004, PASJ, 56, 809

Zhu, L., Qian, S.-B., Mikulášek, Z., et al. 2010, AJ, 140, 215

Zhu, L. Y., Qian, S. B., Soonthornthum, B., He, J. J., & Liu, L. 2011, AJ, 142, 124

Zhu, L.-Y., Qian, S.-B., Zhou, X., et al. 2013, AJ, 146, 28